Electrochimica Acta 370 (2021) 137737

Contents lists available at ScienceDirect

Electrochimica Acta

journal homepage: www.elsevier.com/locate/electacta

Charge effects on the behavior of CTAB adsorbed on Au(111) electrodes in aqueous solutions

José M. Gisbert-González, María V. Oliver-Pardo, Valentín Briega-Martos, Juan M. Feliu, Enrique Herrero*

Instituto de Electroquímica, Universidad de Alicante, Apdo. 99, E-03080 Alicante, Spain

ARTICLE INFO

Article history:
Received 13 October 2020
Revised 2 January 2021
Accepted 3 January 2021
Available online 7 January 2021

ABSTRACT

The behavior of adsorbed CTAB on Au(111) electrodes has been studied using electrochemical and FTIR experiments in different aqueous solutions. The results show that the adsorbed layer is stable in acidic solutions in the whole potential range of study. The observed electrochemical and FTIR behavior is compatible with the formation of a membrane of CTA^+ on the electrode surface with the polar amino groups in contact with the surface. When the electrode charge is negative, the polar groups are attracted to the surface, so that the capacitance of the electrode is smaller than that recorded for the unmodified Au(111) electrode. As the charge becomes positive, the membrane detaches from the surface and water molecules permeate through it, changing the capacitance of the electrode and giving rise to characteristic peaks in the voltammetric profile. At potentials higher than these peaks, the behavior of the electrode is comparable to that observed for the unmodified electrode. The stability of the membrane is facilitated by the incorporation of anions of the supporting electrolyte. Those anions remain on the membrane even when the electrode is transferred to a different solution, as the electrochemical behavior shows.

1. Introduction

Gold nanorods (AuNRs), due to their anisotropy, have very interesting properties, and, for this reason, they have been widely studied because of their potential in biological and biomedical applications [1]. One of the most used synthetic methods for AuNRs employs cetyltrimethylammonium bromide (CTAB), which acts as both a capping and a shaping agent [2-4]. The synthetic method developed by Murphy and El-Sayed groups relies on a seed-mediated growth mechanism, in which the AuNRs grow from spherical Au seeds in CTAB containing solutions [2-4]. This results in nanorods that have (111) facets on both tips and (110) facets on the sides, as revealed by the use of structure sensitive reactions [5]. The final shape of the nanoparticles depends on the ionic strength of the solution and the counterion concentration [3], highlighting the important role of the micellar morphology of CTAB and the surface chemistry [1,4,6-8]. Molecular dynamic simulations have also provided an additional understanding of the growth mechanism [9].

After the synthesis, CTAB remains tightly bonded to the gold surface forming a bilayer structure and the presence of CTAB in solution prevents the agglomeration of the AuNRs. The formation of a CTAB bilayer around the formed AuNRs has been extensively characterized by IR spectroscopy, thermogravimetric analysis, and zeta potential measurements as well as Raman spectroscopy [10-12]. In this bilayer, the bromide anion is adsorbed on the gold surface and interacts with the $(CH_3)_3N^+$functional group of the cetyltrimethylammonium cation (CTA^+). In this configuration, the long hydrophobic alkane chain is pointing to the bulk of the solution, which facilitates the formation of a second layer by the interaction of the alkane chain of other CTA^+ cations. Thus, the hydrophobic alkane chains are located in the central part of the bilayer while the cationic $(CH_3)_3N^+$ groups remain on the external sides of the bilayer. In the growing process, bromide anions have an important role as revealed by observed changes in the shape of the nanoparticles by the addition of iodide [13-15].

The use of CTAB prevents the direct use of the AuNRs in biomedical applications because of the ability of the surfactant to pass through cellular membranes [16]. Therefore, the removal of the CTAB layer from the AuNRs is a required step before its use in physiological environments, which has triggered the study of these processes [3,4,17,18]. Furthermore, as dispersed solutions of CTAB-AuNRs agglomerate when the surfactant concentration is below the critical micelle concentration (~0.1 mM $<$ CTAB $<$ 1 mM), the removal of CTAB requires its exchange

* Corresponding author.
E-mail address: herrero@ua.es (E. Herrero).

https://doi.org/10.1016/j.electacta.2021.137737
0013-4686/

with a physiological-compatible molecule so that aggregation is prevented [19,20].

In order to better understand the interaction of CTAB with gold surfaces, the interaction of CTAB with the Au(111) single crystal electrode has been studied using cyclic voltammetry and FT-IR spectroscopy. The role of electrode charge and electrolyte composition will be studied, which will allow reaching a better comprehension of the behavior of the CTAB adsorbed on AuRNs in aqueous solutions.

2. Experimental

Owing to the low solubility of CTAB in acid solutions, the study of the CTAB interaction with the Au(111) electrode was carried out by immersing the electrode at open circuit into a water solution containing the salt. After rinsing the excess of CTAB with water, the electrode was transferred to the electrochemical cell and immersed at a controlled potential (0.1 V). In the design of the experiments, two facts must be considered. First, the presence of bromide anion can interfere with the CTA^+/Au interaction because bromide anion is strongly adsorbed on the gold electrode [21,22], and, thus, it can compete with the adsorption quaternary ammonium ion. Second, CTAB can form micelles in aqueous solutions and the formation of these micelles can alter the interaction of the species with the gold surface. To avoid that, the concentration of the CTAB in the solutions was below the critical micelle concentration, which is ~1 mM for this case [19,20]. The same procedure was used to modify the electrodes with a cetyltrimethylammonium hydroxide (CTAOH) adlayer.

Au(111) single crystal electrode was prepared using Clavilier's method [23,24] by obtaining firstly a single crystal bead from a fused crystallized ultrapure 0.25 mm diameter gold wire. Secondly, it was mounted in a four-cycle goniometer on an optical bench and, after being properly oriented with laser reflection, cut and polished with diamond paste.

Every electrochemical experiment was set using a glass cell with a reversible hydrogen electrode (RHE), for pH 1, and a Ag/AgCl (1 M KCl) electrode, pH 3, as references. A gold wire was used as counter-electrode. Supporting electrolyte solutions were prepared using concentrated perchloric acid (Merck Suprapur®), sulfuric acid (Merck Suprapur®), and ultrapure water (18.2 MΩ cm, Elga Vivendi). pH 3 solutions also contain sodium fluoride (Merck Suprapur®) to maintain both pH and the ionic strength constant through the experiments. Adsorbates solutions were prepared using CTAB, (BioUltra, for molecular biology, ≥ 99.0%, Sigma-Alrich) and CTAOH (10 wt.% in H_2O, Sigma-Aldrich). All solutions were deaerated with Ar (N50, Air Liquide). Voltammetric experiments were carried out at room temperature using a wave signal generator (EG&G PARC 175), potentiostat (eDAQ 161), and digital recorder (eDAQ e-corder 401) workstation. Cyclic voltammograms were recorded at 50 mV s^{-1}

In situ infrared experiments were carried out using a Nexus 8700 (Thermo Scientific) spectrometer equipped with an MCT-A detector and a wire grid ZnSe polarizer (Pike Tech). The spectroelectrochemical cell was equipped with a prismatic CaF_2 window beveled at 60°, which was placed at the top of a Veemax (Pike Tech.) reflectance accessory. A resolution of 8 cm^{-1} was used to collect every potential-dependent spectra, which is presented in absorbance units (a.u.) as $-\log(R/R_o)$, where R and R_o represent the reflectivities at the sample and reference potentials, respectively. The positive and negative bands correspond, respectively, to the gain and the loss of species at the sample potential with respect to the reference potential. The electrode potential was stepped from the reference to the sample potential collecting 100 interferograms at each potential.

3. Results and discussions

The Au(111) surface presents a complex behavior because it can reconstruct, that is, the top layer can have two different atomic arrangements: the (1 × 1) surface structure (i.e., the expected structure for a (111) face of an fcc metal) and the (22 × √3) reconstructed structure also termed as herringbone reconstruction [25,26]. After flame annealing, the surface is reconstructed. When transferring to electrochemical environments, the stability of these structures depends on the sign of the surface charge and the presence of adsorbates [27,28]. In the absence of adsorbates, the herringbone structure is stable for negatively charged surfaces, whereas the (1 × 1) structure is the surface with the lowest energy for positively charged surfaces [29]. For this reason, the potential at which the surface has zero charge, that is, the potential of zero charge (pzc) is an important value in the analysis of the behavior of these surfaces, whose value for gold is pH-independent. Due to the presence of two different structures, two pzc's can be measured, one of the unreconstructed (1 × 1) structure (pzc_{un}) and one for the reconstructed surface (pzc_r). The values for the pzc_{un} and pzc_r in perchloric acid solutions are 0.43 and 0.52 V vs. RHE, respectively [30-32].

Fig. 1 shows the voltammetric profiles of the Au(111) electrode modified with CTAB in 0.1 M $HClO_4$ and its comparison with that obtained in the absence of CTAB. The selected potential range corresponds to that between the onset of the hydrogen evolution and the surface oxidation. For the unmodified Au(111) electrode in 0.1 M $HClO_4$, the voltammetric profile, obtained after flame annealing and immersion of the electrode at a controlled potential of 0.1 V, shows a broad wave corresponding to the absence of specific adsorption (Fig. 1, black trace). At the immersion potential the surface is reconstructed and potentials above the pzc, the reconstruction is lifted. Due to the absence of specific adsorption, the lifting of the reconstruction does not give rise to a characteristic peak. However, the presence of reconstruction/lifting of the reconstruction phenomena has its effect on the profile, because it is not symmetrical with respect to the x-axis. The lifting of the reconstruction is faster than the reconstruction process [33] so that the surface structure present on the electrode depends on the scan direction, giving rise to the observed asymmetry.

For the Au(111) surface modified with CTAB, the voltammetric profile changes significantly from that obtained in perchloric acid (Fig. 1, red trace). After some cycles, the voltammogram reaches a stable profile. The time for the open circuit adsorption during the adsorption procedure was 30 s in all cases. This adsorption time was selected because for longer times no significant changes were observed in the stable profiles, whereas, for shorter times, the peaks in the profile were less developed. As shown in Fig. 1A, the initial voltammetric profile of the modified electrode changes upon cycling. The broad signal appearing between 0.18 and 0.8 V in the negative scan direction, and the positive currents above 1.1 V in the positive scan direction progressively decrease. In parallel, the peaks in the negative scan direction at 0.9 V become sharper and better defined. After some cycles, a stable voltammogram is obtained (Fig. 1C), which indicates that the adsorption of these species is strong enough in this potential range to reach a stationary behavior and no significant desorption of the adsorbed adlayer is taking place.

One of the possible causes of the initial evolution of the profile for the modified electrode can be related to the presence of bromide anions trapped within the adsorbed layer or adsorbed on it due to coulombic attraction between the anion and the positively charged adlayer. It should be noted that the profile is different from that obtained in the presence of 0.1 mM KBr in solution (Fig. 1B, red trace) [21]. Additionally, when bromide is not present in solution, adsorbed bromide progressively desorbs upon cycling,

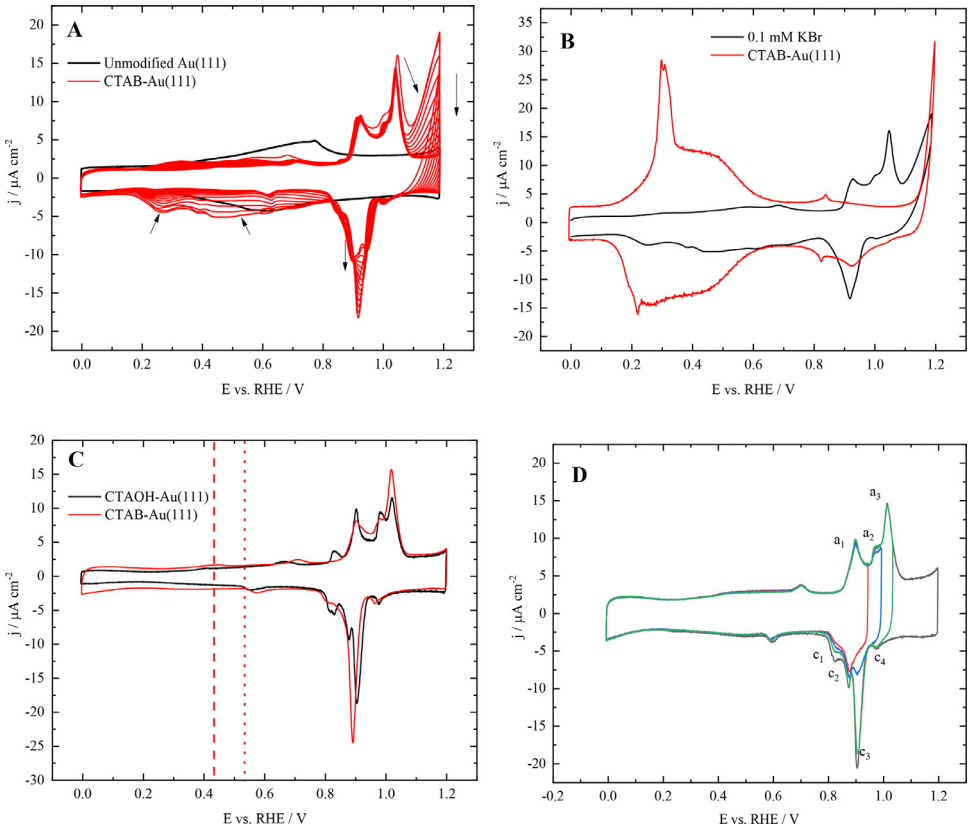

Fig. 1. A) Voltammetric profile for the unmodified Au(111) electrode and the evolution of the profile of the CTAB modified Au(111) electrode upon cycling in 0.1 M $HClO_4$. B) First scan for the CTAB modified Au(111) electrode in 0.1 M $HClO_4$ and for the unmodified Au(111) electrode in 0.1 M $HClO_4$+0.1 mM KBr. C) Voltammetric profiles for the CTAB and CTAOH modified Au(111) electrodes in 0.1 M $HClO_4$. The vertical lines mark the position of the pzc_{un} (dashed line) and pzc_r (dotted line) of the unmodified Au(111) surface. D) Voltammetric profiles for the CTAB modified Au(111) electrode with different upper potential limits in 0.1 M $HClO_4$. Scan rate: 50 mV s^{-1}. (For interpretation of the references to color in this figure, the reader is referred to the web version of this article.)

and the profile evolves from corresponding to bromide solutions to that obtained in the absence of bromide, that is, the one shown in Fig. 1A with black trace. When the first scan for the modified electrode is compared to that obtained in for the bromide containing solution (Fig. 1B), the broad wave observed between 0.18 and 0.8 V has a similar shape to that obtained in KBr solutions, which suggests that bromide is adsorbed on the surface and interacting the adlayer. However, the charge is significantly smaller because the presence of other adsorbed species on the electrode surface (namely CTA^+) diminishes the coverage of adsorbed bromide. As can be observed in this latter figure, bromide is completely desorbed below 0.18 V. In the absence of bromide in solution, at these potentials, bromide anions diffuse from the surface. In the positive scan direction, bromide is partially readsorbed, but after some cycles the bromide concentration at the interphase becomes negligible and a stable profile is obtained. The initial oxidation currents at 1.2 V can also be assigned to the bromide oxidation process. As the amount of adsorbed bromide diminishes, the oxidation currents also diminish. Thus, bromide has been completely desorbed when the stable voltammogram of Fig. 1C is obtained, and the adsorbed layer should only contain CTA^+ cations. To further confirm this hypothesis, the Au(111) electrode was modified with CTAOH, using the same procedure used for the modification with CTAB. For the Au(111) modified by the CTAOH, the stationary behavior is achieved instantly, and as can be seen in Fig. 1C, the stationary voltammetric profile for the CTAOH modified electrode is almost identical to that obtained for the CTAB modified electrode. Thus, it can be concluded that the observed features correspond to the electrochemical behavior of adsorbed CTA^+.

The stable profile of the Au(111) CTAB modified surface shows several peaks in the region between 0.8 and 1.1 V, and below 0.8 V an almost flat response associated with double-layer processes is observed. The currents measured in this region are lower than those measured for in the absence of the adsorbates, which is typical of the presence of a hydrophobic layer. Additionally, owing to the redox stability in the selected potential range of the CTA^+ species, the peaks in the voltammogram should be related to changes in the configuration of the adlayer and not to a redox process of the species [34]. The modifications in the adlayer configuration should lead to changes in the capacitance (and charge) of the electrode, resulting in net charge transfer processes that give rise to peaks. As can be seen in Fig. 1A, the number of peaks in each scan direction is different and peaks are not symmetrical with respect to the x-axis, suggesting a complex change in the structure with some irreversible steps. To get insight into this issue, the profile was recorded with several upper potential limits (Fig. 1D). As can be seen, a_1 peak is closely related to c_2 peak, whereas peak c_3 contains contributions of the processes taking place at a_2 and a_3 peaks. However, the c_1 peak, the one at the lowest potential, is only fully developed when the potential in the positive scan direction is higher than that of peak a_3. This behavior clearly indicates that the transformation in the CTAB layer has an important irreversible component, requiring some time to reach the initial structure.

Another important piece of information regarding the behavior of the formed layer is the enlargement of the potential window to study the region corresponding to the oxide formation/reduction of the Au(111) electrode above 1.2 V (Fig. 2). The CTAB-free Au(111)

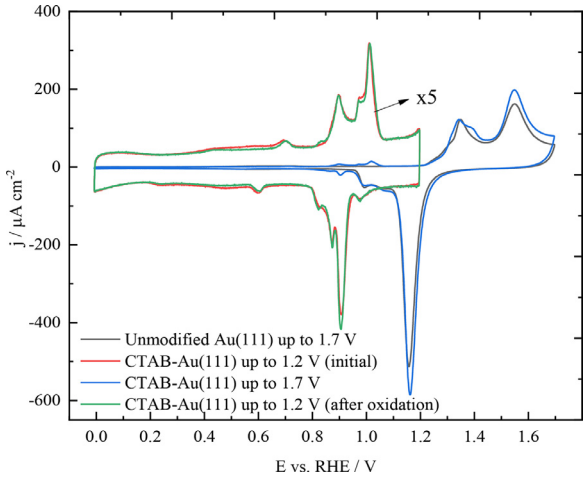

Fig. 2. Voltammetric profiles of the unmodified and CTAB modified Au(111) electrode in 0.1 M $HClO_4$ up to 1.7 V and 1.2 V. The initial profile for CTAB-Au(111) up to 1.2 V and that recorded in the same potential region after the oxidation have been enlarged 10 times to better observe the peaks. Scan rate: 50 mV s^{-1}.

electrode shows two peaks in the positive scan direction related to the Au-OH monolayer formation and the full oxidation of the surface forming an Au-O layer, respectively [35-37]. The negative scan direction only shows a large reduction peak which contains the combined contribution of the reduction of the Au-O to Au in a single process. Interestingly, the profile in this region for the CTAB modified Au(111) electrode is essentially the same as that observed for the unmodified surface. The two characteristic peaks corresponding to the oxidation of the surface appear at the same potentials and the only significant difference is a slight increase in the charge. This increase in charge is also observed in the cathodic peak, which also appears at the same potential. The analogous profile for both electrodes could have been an indication that the oxidation of the surface leads to the desorption of the adsorbed CTA^+ layer. However, the profile between 0 and 1.2 V recorded after this excursion to higher potential values is essentially the same as that recorded initially, which indicates that the CTA^+ layer has remained unaltered after the surface oxidation process. Given that the formation of the Au-OH and Au-O layers requires the presence of water and those oxidation processes are inhibited by the presence of chemically adsorbed molecules, CTA^+ is not bonded to the surface. Thus, it can be proposed that the CTA^+ layer has the behavior of a lipid membrane covering the surface. This membrane allows the permeation of water molecules through it to reach the electrode surface in such a way that the surface can be oxidized at the usual potentials. This hypothesis matches with the biomimetic membranes of phospholipids studied by Lipkowski on gold surfaces [38,39]. Moreover, the separation between the CTA^+ membrane and the Au(111) layer depends on the electrode potential. At potentials below the pzc, the membrane is close to the surface, because the surface charge is negative and attracts the polar groups of the cations so that the double layer capacitance is slightly smaller than that observed for the unmodified Au(111) surface. As the potential increases and the surface charge becomes positive, the polar groups close to the surface start being repelled by the surface positive charge, and additional water molecules penetrate in the region between the surface and the CTA^+ membrane, giving rise to the observed peaks. Under these conditions, where water layers are in contact with the electrode surface, the surface oxidation processes take place under similar conditions to those achieved for the unmodified electrode. Probably, the small changes observed in the oxide region are related to the different activity of the involved species in the region between the membrane and the electrode surface. When the oxides are reduced, and the surface charge becomes negative again, the membrane is attracted to the surface returning to the initial point. It should be noted that the formation of the CTA^+ layer has been observed well below the critical micelle concentration. The formation of full layers on interphases has already been reported for the water-air interphase, where a monolayer is formed for a concentration of CTAB of ca. 1.4 mM [40]. The formation of the full layer is due to the amphiphilic nature of the CTA^+cation. The special environment of this interphase stabilizes the adlayer and thus the polar heads are pointing to the polar side of the interphase (water) whereas the nonpolar tails are pointing to the nonpolar side (air). As aforementioned, the observed behavior, the voltammetric profile of adsorbed CTA^+ on the Au(111) electrode between 0 and 1.2 V is compatible with the formation of a layer. Clearly, when the surface charge is negative, the polar group must be close to the surface, and this interaction helps in the stabilization of the adlayer. This type of behavior is compatible with the formation of a single layer or also the formation of a bilayer, as has been described in the formation of nanoparticles [10-12]. When behavior for $E>1.2$ V in Fig. 2 is considered, the detachment of the layer for $E>1.2$ V and its reattachment when the potential diminishes suggests that the adlayer may have a bilayer structure. The detached monolayer should have some additional stability that would allow its existence in the detached form because the stabilizing force for the formation of the layer (the negative charge of the electrode) has disappeared, and then, the repelled CTA^+ cations would diffuse to the bulk of the solution. Without this additional stabilization force, when the charge becomes negative again, a significant modification of the behavior would have been observed, and the profile would have been closer to that obtained for the unmodified electrode. However, the observed behavior is that the layer at positive surface charges is still stable because no significant loss of the layer is observed, implying that the CTA^+ structure has some additional stability. The most probable configuration in which the layer maintains its structure is the formation of a bilayer, because under these conditions both sides of the layer have a polar nature, with favorable interactions with the polar solvent and anions in solution. However, the formation of a monolayer, with the incorporation of anions that help in the stabilization, or even the formation of a partial bilayer, cannot be discarded. Further works are in progress to fully characterize the layer.

To corroborate that the surface charge is the reason for the changes in the adlayer, the voltammogram of the CTAOH modified Au(111) electrode was recorded in a solution with pH=3. As can be seen in Fig. 3, although there are some differences in the peak definition, the shape of the profiles is, essentially, the same. In fact, when the profiles are plotted in the SHE scale, peaks appear at the same potential. Similar results are obtained with the CTAB modified electrode. As aforementioned, in absence of specific adsorption, the pzc is constant in the SHE, which corroborates that the observed processes in the adlayer are driven by the surface charge of the electrode.

To further analyze this process, FTIR experiments have been carried out (Fig. 4). In the first set of spectra, the potential is increased from 0.1 V, whose spectrum is taken as reference, up to 1.2 V, and the spectra are taken every 0.10 V. As can be seen, a negative band at 2905 cm^{-1} starts developing from 0.6 V in parallel with the growth of a weak positive band at 1381 cm^{-1}. This potential coincides with the onset potential for the peaks observed in the voltammetric profile, which clearly indicates that these bands correspond to the processes taking place in these peaks. The band at 1381 cm^{-1} can be assigned to the symmetric bending mode of -CH_3 groups [41] whereas the band at 2905 cm^{-1} corresponds to the Fermi resonance of the symmetric stretching of the -CH_2 groups [40,42]. In the negative scan direction, when the reference spec-

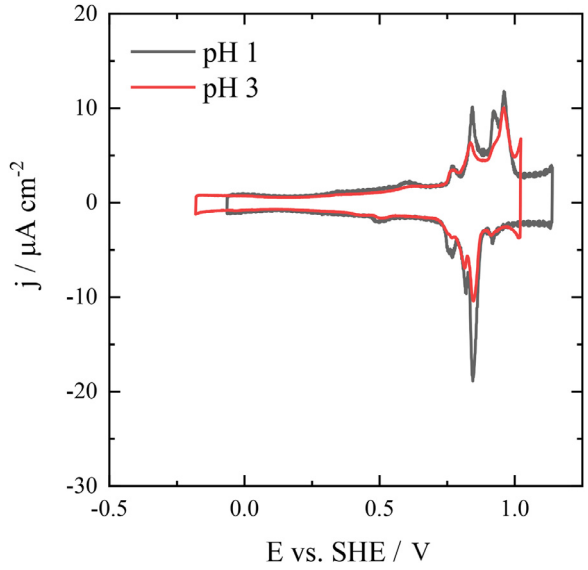

Fig. 3. Voltammetric profiles of the Au(111) electrode in the presence of adsorbed CTAOH in solutions with pH≈1 (0.1 M $HClO_4$) and pH≈3 (2.99 × 10^{-2} M $HClO_4$ + 4.84 × 10^{-2} M NaF). Scan rate: 50 mV s^{-1}.

trum is taken at 1.2 V, the evolution of these bands is the opposite. Due to the reflection of the p-polarized FTIR signal on the surface, there is an increase in the field that the groups close to the surface are observing allowing to detect adsorbed species. The increase of the band related to the symmetric bend of $-CH_3$ groups can be related to the formation of hydrogen bonds between the $-CH_3$ groups and water and the change in orientation with respect to the gold surface [41], as has been already reported for gold nanorods. This increase in the band intensity is consistent with the detachment of the CTA^+ cations from the surface and the permeation of water to fill the gap created between the layer and the electrode surface. On other hand, the diminution of the bands associated with $-CH_2$ groups should be related to conformational changes in the alignment of the hydrocarbon chain in the nonpolar tail of the cation as the membrane detaches.

Given that the interaction of the CTA^+ adlayer with the surface is purely electrostatic, the presence of strongly adsorbing anions in the electrolyte can modify these interactions. To investigate this point, the profiles were recorded in 0.1 M H_2SO_4. Fig. 5A shows the voltammetric profile of the unmodified (111) electrode and the evolution upon cycling of the CTAB modified electrode with a sharp peak with a pre-shoulder. For the unmodified electrode, sulfate adsorption starts at ca. 0.3 V and give rise to a peak at 0.59 V due to the lifting of the reconstruction in the positive scan direction [28]. The sharp pair of peaks at ca. 1.1 V is due to the formation of and disorder/order transition in the adsorbed sulfate layer [43]. In the case of the CTAB modified electrode, the initial positive scan direction resembles that obtained in perchloric acid. The peak appears at a lower potential than that recorded in perchloric acid probably because of the presence of sulfate, which adsorbs strongly on the electrode surface and shifts the pzc to lower potential values. However, in the negative scan direction, the peaks are smaller and less developed. The presence of a strongly adsorbed sulfate layer, which is adsorbed above 0.3 V, prevents the interaction of the CTA^+ adlayer with the surface. As the cycling progresses, the previously described set of peaks diminish progressively until a stable profile is reached (Fig. 5B). This profile is very similar to that recorded in the absence of the adlayer. In fact, the peaks related to the disorder/order transition for the sulfate adlayer are still visible. The comparable profile to that measured for the unmodified electrode would suggest that the CTA^+ adlayer would have been almost completely desorbed. However, the profile below 0.4 V is different, which is a clear indication the adlayer is still present.

Further proofs of the presence of the CTA^+ layer can be obtained if the scan is extended up to 1.7 V. Fig. 6 shows the profiles of the unmodified (red trace) and the CTAB modified Au(111) (blue trace) electrode in 0.1 M H_2SO_4. As can be seen, the main peak for the oxidation of the Au(111) surface for the modified electrode in 0.1 M H_2SO_4 is sharper and appears at higher potential values than that recorded for the unmodified electrode. This type of behavior is a clear indication that the adsorption of sulfate is stronger for the

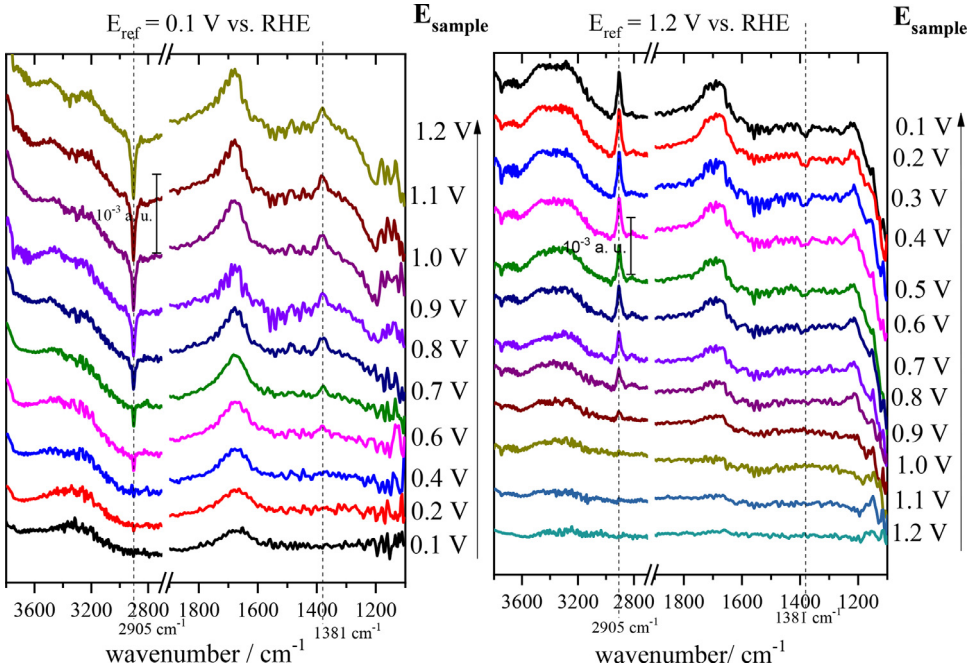

Fig. 4. FTIR spectra for the CTAB modified Au(111) electrode in 0.1 M $HClO_4$ for the (A) positive and (B) negative scan directions. The reference spectrum is taken at the initial potential of each scan direction.

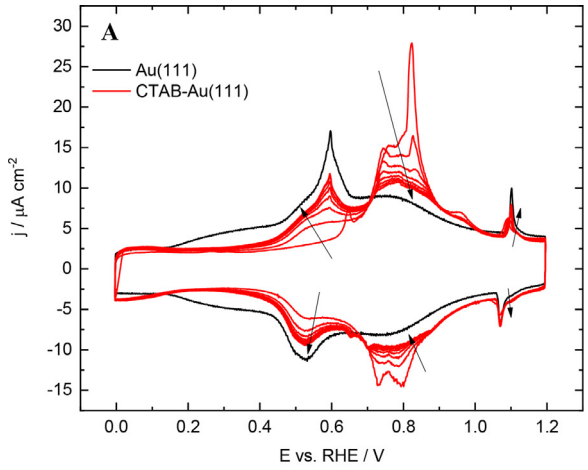

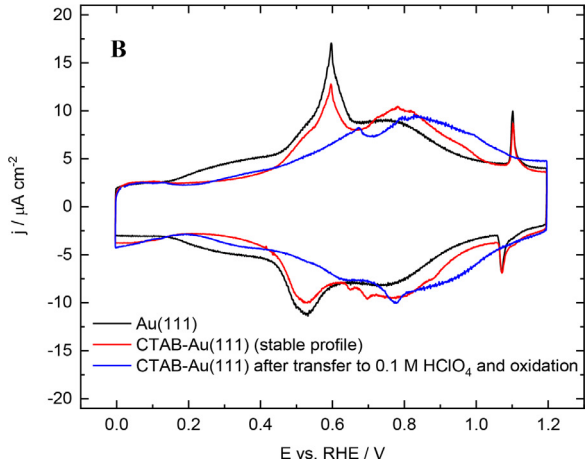

Fig. 5. (A)Voltammetric profiles of the Au(111) electrode in 0.1 M H_2SO_4 for the unmodified and CTAB modified Au(111) electrode. The arrows indicate the evolution of the profile for the modified electrode upon cycling. (B) Comparison of the stable profiles for the unmodified and CTAB modified Au(111) electrode in 0.1 M H_2SO_4 and that obtained after the transfer of the CTAB modified Au(111) electrode from 0.1 M H_2SO_4 to 0.1 M $HClO_4$ and its oxidation. Scan rate: 50 mV s^{-1}. (For interpretation of the references to color in this figure, the reader is referred to the web version of this article.)

CTAB modified electrode, which points out that adsorbed sulfate interacts with the positively charged adlayer hindering its desorption. This fact implies that the CTA^+ layer is interacting with the adsorbed sulfate creating a structured interphase composed of an adsorbed sulfate layer in contact with the electrode surface and a CTA^+ layer. The adsorption of the sulfate layer, in this case, is stronger than that observed for a pure sulfate layer.

The existence of the structured interphase in which the CTA^+ layer is stabilized by the presence of anions can also be corroborated by transfer experiments. For this experiment, the CTAB modified electrode is initially characterized in 0.1 M H_2SO_4. After the stable profile of Fig. 5A is obtained, the electrode is emersed from the cell at 1.2 V and transferred to a cell containing 0.1 M $HClO_4$, where it is immersed at 1.2 V. Starting from this potential value, a voltammetric scan is registered in the oxidation region up to 1.7 V. As can be seen in Fig. 6, green trace, the oxidation profile obtained after the transfer to the $HClO_4$ solution is very different from that obtained previously in the $HClO_4$ solution (Fig. 2). In fact, the peak distribution and the charges are almost the same as those

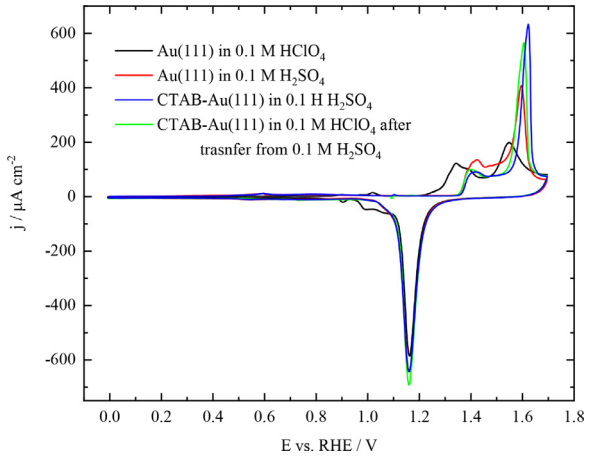

Fig. 6. Voltammetric profiles of the unmodified and CTAB modified Au(111) electrode in different conditions. Scan rate: 50 mV s^{-1}. (For interpretation of the references to color in this figure, the reader is referred to the web version of this article.)

recorded previously in for the CTAB modified electrode in H_2SO_4 (Fig. 6, blue trace) which clearly indicates that the presence of the structured interphase has remained unaltered after the transfer to the perchloric acid solution. Sulfate anions are still present in the electrolyte interphase close to the electrode surface so that the electrochemical response is still that typical of sulfuric acid solutions. Moreover, the voltammogram in the region $E<1.2$ V still has the characteristics of the presence of a sulfate layer (Fig. 5B, blue trace), although the peaks are displaced to slightly higher potential values probably due to the absence of sulfate in the supporting electrolyte.

4. Conclusions

The electrochemical and FTIR results explain the stability of the CTAB layers on the gold surfaces. The results presented here suggest that a layer of CTA^+ cations is formed after the transfer from the solution containing CTAB. This layer attaches/detaches from the surface depending on the electrode charge. At negative charges, the amino polar groups are attracted to the surface, whereas positive charges repel the membrane and water molecules intercalate between the electrode surface and the membrane. For this reason, the oxidation of the surface gives rise to peaks that are comparable to those obtained in the absence of the membrane, because at these potentials the membrane is detached from the surface. Despite the movement of the membrane, it is stable in acidic media. Due to the strong repulsive forces between the CTA^+ chains within the membrane, its stabilization is accomplished by the interaction with the anions of the supporting electrolyte, as the transfer experiments from sulfuric to perchloric solutions demonstrate.

Authors contribution

All authors have contributed equally to this manuscript.

Declaration of Competing Interest

The authors declare that they have no known competing financial interests or personal relationships that could have appeared to influence the work reported in this paper.

Acknowledgments

Financial support from Ministerio de Ciencia e Innovación (Project PID2019-105653GB-100) and Generalitat Valenciana (Project PROMETEO/2020/063) is acknowledged.

References

[1] J. Perez-Juste, I. Pastoriza-Santos, L.M. Liz-Marzan, P. Mulvaney, Gold nanorods: synthesis, characterization and applications, Coor, Chem. Rev. 249 (2005) 1870–1901.
[2] A. Gole, C.J. Murphy, Seed-mediated synthesis of gold nanorods: role of the size and nature of the seed, Chem. Mater. 16 (2004) 3633–3640.
[3] C.J. Murphy, T.K. Sau, A.M. Gole, C.J. Orendorff, J. Gao, L. Gou, S.E. Hunyadi, T. Li, Anisotropic metal nanoparticles: synthesis, assembly, and optical applications, J. Phys. Chem. B 109 (2005) 13857–13870.
[4] B. Nikoobakht, M.A. El-Sayed, Preparation and growth mechanism of gold nanorods (NRs) using seed-mediated growth method, Chem. Mater. 15 (2003) 1957–1962.
[5] J. Hernández, J. Solla-Gullón, E. Herrero, A. Aldaz, J.M. Feliu, Characterization of the surface structure of gold nanoparticles and nanorods using structure sensitive reactions, J. Phys. Chem. B 109 (2005) 12651–12654.
[6] K. Park, L.F. Drummy, R.C. Wadans, H. Koerner, D. Nepal, L. Fabris, R.A. Vaia, Growth mechanism of gold nanorods, Chem. Mater. 25 (2013) 555–563.
[7] S. Si, C. Leduc, M. Delville, B. Lounis, Short gold nanorod growth revisited: the critical role of the bromide counterion, ChemPhysChem 13 (2012) 193–202.
[8] X. Ye, L. Jin, H. Caglayan, J. Chen, G. Xing, C. Zheng, V. Doan-Nguyen, Y. Kang, N. Engheta, C.R. Kagan, C.B. Murray, Improved size-tunable synthesis of monodisperse gold nanorods through the use of aromatic additives, ACS Nano 6 (2012) 2804–2817.
[9] G. Grochola, I.K. Snook, S.P. Russo, Computational modeling of nanorod growth, J. Chem. Phys. 127 (2007) 195707.
[10] C.J. Murphy, L.B. Thompson, A.L. Alkilany, P.N. Sisco, S.P. Boulos, S.T. Sivapalan, J.A. Yang, D.J. Chernak, J. Huang, The many faces of gold nanorods, J. Phys. Chem. Lett. 1 (2010) 2867–2875.
[11] L. Shao, H. Chen, Q. Li, J. Wang, Gold nanorods and their plasmonic properties, Chem. Soc. Rev. 42 (2012) 2679.
[12] D. Nepal, K. Park, R.A. Vaia, High-yield assembly of soluble and stable gold nanorod pairs for high-temperature plasmonics, Small 8 (2012) 1010–1020.
[13] D.K. Smith, N.R. Miller, B.A. Korgel, Iodide in CTAB prevents gold nanorod formation, Langmuir 25 (2009) 9518–9524.
[14] J.E. Millstone, W. Wei, M.R. Jones, H. Yoo, C.A. Mirkin, Iodide ions control seed-mediated growth of anisotropic gold nanoparticles, Nano Lett. 8 (2008) 2526–2529.
[15] N. Garg, C. Scholl, A. Mohanty, R. Jin, The role of bromide ions in seeding growth of Au nanorods, Langmuir 26 (2010) 10271–10276.
[16] L. Wang, X. Jiang, J. Ji, R. Bai, Y. Zhao, X. Wu, C. Chen, Surface chemistry of gold nanorods: origin of cell membrane damage and cytotoxicity, Nanoscale 5 (2013) 8384–8391.
[17] F. Scaletti, S.K. Chang, L. Messori, M.R. Vincent, Rapid purification of gold nanorods for biomedical applications, MethodsX 1 (2014) 118–123.
[18] R. del Caño, J.M. Gisbert-Gonzalez, J. Gonzalez-Rodriguez, S.-.O. G., R. Madueño, M. Blazquez, T. Pineda, Effective replacement of cetyltrimethylammonium bromide (CTAB) by mercaptoalkanoic acids on gold nanorod (AuNR) surfaces in aqueous solutions, Nanoscale 12 (2020) 658–668.
[19] B.C. Rostro-Kohanloo, L.R. Bickford, C.M. Payne, E.S. Day, L.J.E. Anderson, M. Zhong, S. Lee, K.M. Mayer, T. Zal, L. Adam, C.P.N. Dinney, R.A. Drezek, J.L. West, J.H. Hafner, The stabilization and targeting of surfactant-synthesized gold nanorods, Nanotechnology 20 (2009) 434005.
[20] S. Lee, L.J.E. Anderson, C.M. Payne, J.H. Hafner, Structural transition in the surfactant layer that surrounds gold nanorods as observed by analytical surface-enhanced raman spectroscopy, Langmuir 27 (2011) 14748–14756.
[21] Z.C. Shi, J. Lipkowski, S. Mirwald, B. Pettinger, Electrochemical and second harmonic generation study of bromide adsorption at the Au(111) electrode surface, J. Chem. Soc. Faraday Trans. 92 (1996) 3737–3746.
[22] O.M. Magnussen, B.M. Ocko, J.X. Wang, R.R. Adzic, In-situ X-ray diffraction and STM studies of bromide adsorption on Au(111) electrodes, J. Phys. Chem. 100 (1996) 5500–5508.
[23] J. Clavilier, R. Faure, G. Guinet, R. Durand, Preparation of monocrystalline Pt microelectrodes and electrochemical study of the plane surfaces cut in the direction of the {111} and {110} planes, J. Electroanal. Chem. 107 (1980) 205–209.
[24] A. Rodes, E. Herrero, J.M. Feliu, A. Aldaz, Structure sensitivity of irreversibly adsorbed tin on gold single-crystal electrodes in acid media, J. Chem. Soc. Faraday Trans. 92 (1996) 3769–3776.
[25] U. Harten, A.M. Lahee, J.P. Toennies, C. Wöll, Observation of a soliton reconstruction of Au(111) by high-resolution helium-atom diffraction, Phys. Rev. Lett. 54 (1985) 2619–2622.
[26] S. Narasimhan, D. Vanderbilt, Elastic stress domains and the herringbone reconstruction on Au(111), Phys. Rev. Lett. 69 (1992) 1564–1567.
[27] J.M. Gisbert-Gonzalez, W. Cheuquepán, A. Ferré-Vilaplana, J.M. Feliu, E. Herrero, Citrate adsorption on gold: understanding the shaping mechanism of nanoparticles, J. Electroanal. Chem. (2020) 114015.
[28] Z. Shi, J. Lipkowski, M. Gamboa, P. Zelenay, A. Wieckowski, Investigations of SO 4 2- adsorption at the Au(111) electrode by chronocoulometry and radiochemistry, J. Electroanal. Chem. 366 (1994) 317–326.
[29] X. Gao, A. Hamelin, M.J. Weaver, Atomic relaxation at ordered electrode surfaces probed by sanning tunneling microscopy: Au(111) in aqueus solution compared with ultrahigh-vacuum enviroments, J. Chem. Phys. 95 (1991) 6993–6996.
[30] U.W. Hamm, D. Kramer, R.S. Zhai, D.M. Kolb, The pzc of Au(111) and Pt(111) in a perchloric acid solution: an ex situ approach to the immersion technique, J. Electroanal. Chem. 414 (1996) 85–89.
[31] D.M. Kolb, J. Schneider, Surface reconstuction in electrochemistry: Au(100)-(5x20), Au(111)-(1x23) and Au(110)-(1x2), Electrochim. Acta 31 (1986) 929–936.
[32] X. Gao, A. Hamelin, M.J. Weaver, Atomic relaxation at ordered electrode surfaces probed by scanning tunneling microscopy: Au(111) in aqueous solution compared with ultrahigh-vacuum environments, J. Chem. Phys. 95 (1991) 6993–6996.
[33] X. Gao, S.C. Chang, X. Jiang, A. Hamelin, M.J. Weaver, Emergence of atomic level structural information for oredered metal-solution interfaces: some recent contributions from in- situ infrared spectroscopy and scanning tunneling microscopy, J. Vac. Sci. Technol. A 10 (1992) 2972.
[34] E. Nouri-Nigjeh, M.P. de Vries, A.P. Bruins, R. Bischoff, H.P. Permentier, Electrochemical oxidation of quaternary ammonium electrolytes: unexpected side reactions in organic electrochemistry, Electrochem. Commun. 21 (2012) 54–57.
[35] H. Angersteinkozlowska, B.E. Conway, A. Hamelin, L. Stoicoviciu, Elementary steps of electrochemical oxidation of single-crystal planes of Au .2. A chemical and structural basis of oxidation of the (111) plane, J. Electroanal. Chem. 228 (1987) 429–453.
[36] H. Angerstein-Kozlowska, B.E. Conway, A. Hamelin, L. Stoicoviciu, Elementary steps of electrochemical oxidation of single-crystal planes of Au .1. Chemical basis of processes involving geometry of anions and the electrode surfaces, Electrochim. Acta 31 (1986) 1051–1061.
[37] S. Strbac, A. Hamelin, R.R. Adzic, Electrochemical indication of surface reconstruction of (100), (311) and (111) gold faces in alkaline solutions, J. Electroanal. Chem. 362 (1993) 47–53.
[38] J. Lipkowski, Building biomimetic membrane at a gold electrode surface, Phys. Chem. Chem. Phys. 12 (2010) 13853–14368.
[39] J. Lipkowski, Biomimetic membrane supported at a metal electrode surface: a molecular view, in: A. Iglič, C.V. Kulkarni (Eds.), Advances in Planar Lipid Bilayers and Liposomes, Elsevier, 2014, pp. 1–49.
[40] R.A. Campbell, S.R.W. Parker, J.P.R. Day, C.D. Bain, External reflection FTIR spectroscopy of the cationic surfactant hexadecyltrimethylammonium bromide (CTAB) on an overflowing cylinder, Langmuir 20 (2004) 8740–8753.
[41] B. Nikoobakht, M.A. El-Sayed, Evidence for bilayer assembly of cationic surfactants on the surface of gold nanorods, Langmuir 17 (2001) 6368–6374.
[42] R. Lu, W. Gan, B.-h. Wu, Z. Zhang, Y. Guo, H.-f. Wang, C−H stretching vibrations of methyl, methylene and methine groups at the vapor/alcohol (n = 1−8) interfaces, J. Phys. Chem. B 109 (2005) 14118–14129.
[43] O.M. Magnussen, J. Hageböck, J. Hotlos, R.J. Behm, In situ scanning tunnelling microscopy observations of a disorder-order phase transition in hydrogensulfate adlayers on Au(111), Faraday Discuss. 94 (1992) 329–338.